GUIdEStaR (G-quadruplex, uORF, IRES, Epigenetics, Small RNA, Repeats), the integrated metadatabase in conjunction with neural network methods

Jee Eun Kang[1 §]

[1]BK21 FOUR R&E center for life sciences, Korea University, Seoul 02841, South Korea

[§] Corresponding author

Email addresses:

JEK: jekang_39@yahoo.com

Abstract

GUIdEStaR integrates existing databases of various types of G-quadruplex, upstream open reading frame (uORF), Internal Ribosome Entry Site (IRES), methylation to RNA and histone protein, small RNA, and repeats. The database consists of approx. 40,000 genes and 320,000 transcripts. An mRNA transcript is organized into 5 regions (5'UTR, 3'UTR, exon, intron, and biological region) where each region contains the presence/absence information of 169 different types of elements. Recently, artificial intelligence (AI) based analysis of sequencing data has been gaining popularity in the area of bioinformatics. GUIdEStaR generates a dataset that can be used as an input to AI methods, and comes with example Java codes for data retrieval. Here, we demonstrate the database usage with three neural network classification studies- 1) small RNA study for classifying transcription factor (TF) genes as either TF mediated by small RNA originated from SARS-CoV-2 or one by human microRNA (miRNA), 2) cell membrane receptor study for classifying the receptors as either virus interacting receptor or non-interacting one, and 3) nonsense mediated mRNA decay (NMD) study for classifying cell membrane and nuclear receptors as either receptor targeted by NMD or that of non-target. GUIdEStaR is freely available at www.guidestar.kr and https://sourceforge.net/projects/guidestar.

Introduction

Varied types of sequence compositions, structures, and epigenetic modifications are interwoven for orchestrated gene function. Here, we introduce the metadatabase, GUIdEStaR that integrates existing databases of **G**-quadruplex (GQ) provided by Chariker et al., **u**ORF from uORF-Tools, **I**RES from IRESbase, **E**pigenetic modification from Met-DB V2.0 and Choi et al., **S**mall RNA from DASHR 2.0, and **R**epeats from RepeatMasker into a single resource [1-7]. GUIdEStaR provides the presence/absence information of 845 elements per transcript and consists of approx. 40,000 genes and 320,000 transcripts.

These elements are interdependent in controlling gene regulation through functional interactions. GQ, which is a topological change required of numerous conserved regulatory elements, has become increasingly important in recent years as the mutual dependency between GQ and epigenetic modification has been unveiled [8,9]. uORFs with a conserved peptide are often cleaved by miRNA for controlling the translation of their main ORFs that are frequently regulatory genes such as transcription factors and 5' signal transduction factors [10-12]. They, together with IRES are known to select a specific RNA variant for translation and cellular localization [13]. Genes containing small RNA loci implicate various functions in cellular signaling, and the binding affinity of small RNA is regulated by epigenetic modification [14-16]. Repeats function as a gene regulator; for example, downregulation caused by intronic repeats can be suppressed by epigenetic modification [17,18]. Finally, epigenetic modification regulates gene expression, biogenesis of miRNA, and suppression of transposable elements [19,20].

Here, we demonstrate three studies to show how to chain GUIdEStaR with neural network methods- classification and attribute selection. The first study was to classify human transcription factors (TFs) as either one mediated by small RNA that has its origin in coronavirus or one by human miRNA [21, 22]. In addition to GUIdEStaR, the datasets included log base2 (fold change in gene level abundance) (log base2 FC) information in eight different cell types (ciliated cells, basal cells, club cells, goblet cells, neuroendocrine cells, ionocytes, and tuft cells) from single-cell (sc) RNA-seq [23,24]. The top ranked attributes were putative

G-quadruplex-forming sequence (PU1-*), rRNA, short interspersed nuclear element (SINE) family, long interspersed nuclear element (LINE) family, epigenetic modification- m^6A target sites of WTAP, METTL3, and FTO, and log base2 FC information. The binary neural network models achieved the average accuracy of 90% (Table 1, Table S1, supplementary data).

The second study was to classify cell membrane receptors as either one with virus interaction or one with no interaction. Recent studies documented that protease functioned as co-receptor to facilitate virus entry and interacted with methyltransferase to modulate the activation of a receptor [25,26]. It was reported that cell membrane receptor bound by a growth factor increased transcript abundances of specific TFs and proteases by the intracellular signaling cascades [27,28]. In addition to data from GUIdEStaR, we included the sign functions of the log base2 FCs of diverse TFs, growth factors, proteases, and methyltransferases. Interestingly, the top attributes that contributed the most to the classification were binary data based upon the sign functions of log base2 FCs in ciliated cells and SINE-mammalian-wide interspersed repeats (MIR). The average accuracy of the binary classifiers was 72%. The third study was to classify the cell membrane and nuclear receptors as either that of nonsense mediated mRNA decay (NMD) target or that of non-NMD target. The top 10 attributes included GQ (4:1:1), long term repeat (LTR) family, Tc1-Mariner-like elements (DNA-TcMar), LINE-L2, DNA-hAT-Blackjack, and RNA m^6A modification target sites of METTL14 and YTHDF1, where the GQ format x:y:z was interpreted as “x represents the number of guanine tracts, y represents the number of locations at which a G4 could form, and z represents the number of G4 that could form simultaneously in the sequence” [1]. The average accuracy was 72%. GUIdEStaR is freely available to academic and non-academic users at www.guidestar.kr and https://sourceforge.net/projects/guidestar.

Materials and Methods

Database Integration:

Ensembl gff file (hg38 version: 101) was used to determine the transcript location. A transcript ID (Ensembl ENST) file consists of 845 attributes in the case of mRNA, where each of 5' UTR, 3' UTR, exon, intron, and biological region comprises 169 presence/ absence

attributes in the order mentioned above. For example, the first 169 presence/absence information of GUIdEStaR were from 5' UTR region of a transcript: 25 different types of GQ provided by Chariker et al., uORF from uORF-Tools, IRES from IRESbase, epigenetic modifications to the histone protein H3 provided by Choi et al., target sites of RNA N^6-methyl-adenosine (m^6A) writers (KIAA1429, METTL3, METTL14, and WTAP), readers (YTHDC1 and YTHDF1), and eraser (FTO) in 5' UTR, CDS, 3' UTR, mRNA, lncRNA, sncRNA, tRNA, miRNA, and tumor suppressor miRNA (miRNATS) from Trew database of Met-DB V2.0, 13 different types of small RNAs from DASHR 2.0, and 64 different types of repeats from RepeatMasker. If a transcript is an lncRNA, it contains three regions in the order of exon, intron, and biological region. G-quadruplex, uORF, IRES, small RNA, and repeats have different binary values per region and per transcript, while epigenetic information (Trew database) has a different value per region and per gene. Epigenetic modifications to the histone protein H3 (H3K27me3 and H3K4me3) have the same values in all five regions of a gene. In three example studies, example Java codes created datasets that were readily inputted to neural network methods (Supplementary Data: JAVA_code_examples).

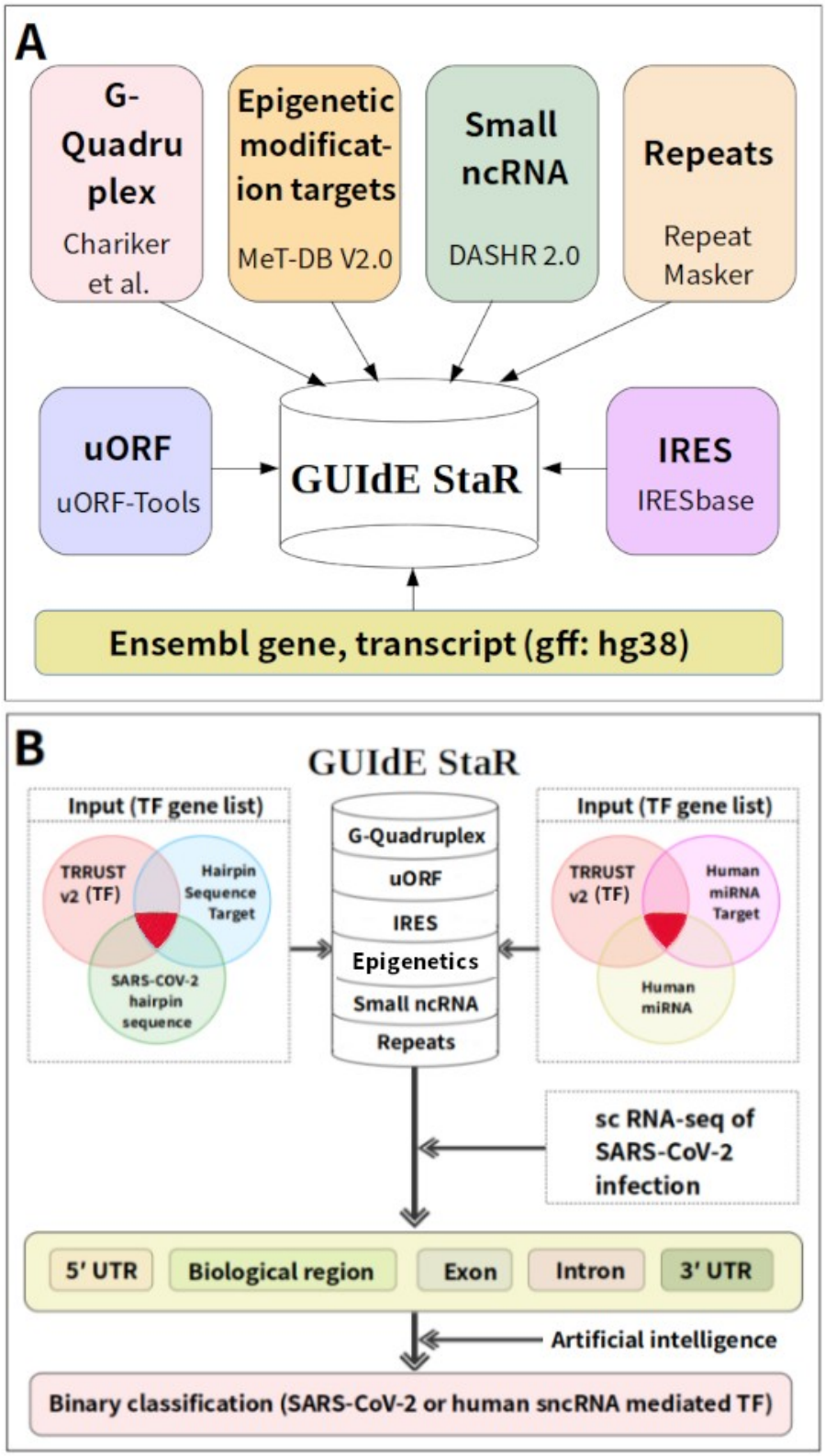

Fig1. (A) Data integration of GUIdEStaR. (B) Workflow of the usage demonstration- small RNA study

Database usage demonstration:

In all three studies, we retrieved the presence/ absence data of 845 attributes of all mRNA transcripts belonging to a gene from GUIdEStaR, splitted them into 5' UTR, 3' UTR, exon, intron, and biological region, set an attribute to have the value- “true” if the attribute was present in at least one transcript, and included additional scRNA-seq data of SARS-CoV-2 infection- log base2 FC information in eight different cell types (Supplementary Data: neural_network_inputs) [24]. We built binary classifiers using Weka’s meta classifier, MultiClassClassifierUpdateable with default values (method: against-all, random number seed: 1, base classifier: Stochastic Gradient Descent (SGD), loss function: hinge loss (SVM), learning rate: 0.01, lambda: 1.0E-4, epochs: 500, epsilon: 0.001, normalization) [30]. Resampling preprocessing step was applied in prior to running each classifier due to the small sample number. We assessed the contribution of an attribute to the classification accuracy, using CorrelationAttributeEval with default values for all parameters [30]. For receptor studies, additional 1048 binary values were generated by the same sign function that evaluated whether x and y had the same sign where x and y were the log base2 FCs of a receptor gene (subject) and of an attribute- gene family (factor) in a dataset. An attribute gene belonged to one of the following families: growth factor families (bone morphogenetic protein, ciliary neurotrophic factor, LIF, interleukin, epidermal growth factor, erythropoietin, fibroblast growth factor, GDNF family, IGF like family, macrophage, nerve growth factor, neurotrophin, platelet derived growth factor, T cell, megakaryocyte, transforming, and tumor necrosis factor), TF families (AP-2, ARID/BRIGHT, AT hook, BED ZF, Brinker, C2H2 ZF, and other 67 families), proteases (peptidase, transamidase, retropepsin, separase, elastase, glutamyltransferase, and other 51 families), 8 different types of histone methyltransferases (ASH1L, DOT1L, EHMT1, MLL, NSD1, PRDM2, SET, and SETMAR, and other 29 genes), 4 different types of DNA methyltransferases (DNMT1, TPMTP3, DPY30, MGMT, and other 13 genes), 3 different types of RNA methyltransferases (METTL14, NSUN2, TRDMT1, VIRMA, and 87 other genes), or other 10 different types of methylation enzymes (ICMT, SHMT1P1, PCMT1,

CARM1P1, EHMT1, CMTR1, AP000812, ARMT1, AS3MT, AC006022, and other 103 genes) (Table S2, JAVA_code_examples: input_files_to_codes).

Small RNA study:

Small RNAs originated from SARS-CoV-2 and from human were selected based on the study of Demirci et al. [31]. TF target genes mediated by SARS-CoV-2 encoded small RNAs were selected based on the same study, while those mediated by human miRNA were based on miRDB and TRRUST v2 (Supplementary Data: neural_network_inputs: small_RNA) [32,33].

Cell membrane receptor with virus interaction study:

Cell membrane receptors that were known to bind to growth factors were selected based upon Wikipedia (https://en.wikipedia.org/wiki/Cell_surface_receptor). Among the receptors, those interacting with different types of viruses were selected based upon the database, Viral Receptor (Supplementary Data: neural_network_inputs: receptor_virus_non_virus) [34].

Cell membrane and nuclear receptors of NMD target vs. non-target:

Nuclear receptors were selected based on wikipedia (https://en.wikipedia.org/wiki/Nuclear_receptor). Genes containing NMD-target transcripts were selected based upon gene annotation of the gff file from Ensembl Homo sapiens 101 (Supplementary Data: neural_network_inputs: receptor_NMD_non_NMD).

Results and Discussion

The accuracies of binary classifiers estimated with cross-validation (folds=10) are shown in Table 1 (Table S1, Supplementary Data: neural_network_outputs). The top 10 attributes in the small RNA study were GQ (PU1-*), target sites of m^6A writer and eraser (WTAP target site overlapping with sncRNA, WTAP with 5' UTR, FTO with 5' UTR, WTAP with lncRNA), repeats (SINE-tRNA-Deu, SINE-5S-Deu-L2), and log base2 FC data (basal cells, tuft cells, and ciliated cells of infected/bystander cell data) (Supplementary data).

Table 1. Accuracies of binary classifiers

Accuracy	5'UTR	Biol. Reg.	Exon	Intron	3'UTR
Small RNA targets (virus origin vs.- human origin)	88 %	88 %	93 %	91 %	89 %

Receptors with virus interaction vs. receptors without virus interaction	73 %	68 %	72 %	78 %	71 %
Cell membrane receptors vs. nuclear receptors	83 %	80%	85 %	88 %	82 %
Receptors of NMD target vs. receptors of non-NMD target	75 %	70%	69 %	77 %	70 %

It was interesting to find that the top 10 attributes in the cell membrane receptor with virus interaction study were gene expression comparisons only from ciliated cells: sign functions of log base2 FCs of the following families- protease family (nicalin), transcription factor family (NFX), and growth factor families (erythropoietin, epidermal growth factor, ciliary neurotrophic factor, fibroblast growth factor, GDNF family, neurotrophin, T cell, platelet derived growth factor). It was consistent with the scRNA-seq study that ciliated cells were mainly the targets of SARS-COV-2 infection [24]. Top 10 attributes in the receptors of NMD target study were repeats (LTR, DNA-TcMar, LTR-endogenous retrovirus1 (LTR-ERV1), LINE-L2, DNA-hAT-Blackjack, LTR-ERVL-MaLR), RNA, and target sites of m^6A writer and reader (METTL14 target site overlapping with mRNA, METTL14 with 3' UTR, YTHDF1 with mRNA).

Although omics data availability rapidly increases, the bottleneck is the lack of bioinformatics software and databases that provide users with a convenient means to extract meaningful information that conveys valuable knowledge. GUIdEStaR provides an easy access to key elements of a transcript/gene with a single inquiry. Due to the highly dynamic nature of epigenetic modification, neural network methods such as association rule may reveal useful insights for studying requirements interdependencies of the elements in a transcript and a link between particular features and a specific condition of cellular microenvironment.

Conclusions

Despite the importance of G-quadruplex, uORF, IRES, Epigenetics, Small RNA, and Repeats, no single resource is available for accessing these information with transcript/gene query. GUIdEStaR is the first database that integrates the information into a single data bank.

Artificial intelligence methods are nowadays widely used in various fields of biological sciences. GUIdEStaR that generates a binary dataset- an input to neural network methods will simplify the application of artificial intelligence methods. Here, we also provide a glimpse of the database usage in conjunction with neural network methods; we demonstrate the feasibility of using these elements as discriminative features to identify human TFs and cell membrane receptors that interact with sequences of viral origin in addition to the identification of receptors of NMD target. We plan to integrate sequence composition and epigenetic modification at single nucleotide resolution into the current GUIdEStaR to provide a useful insight for studying the molecular mechanisms underlying the requirements interdependencies in gene regulation.

Availability

GUIdEStaR, example Java codes for data retrieval, and supplementary materials are available at www.guidestar.kr and https://sourceforge.net/projects/guidestar/.

Conflicts of Interest

The authors declare no competing interests.

Funding Statement

This work was supported by grants from National Research Foundation of Korea (NRF-2020R1A6A3A01099714).

Supplementary Materials

- Table S1. Evaluation of the binary classifiers.
- Table S2. Families of TF, histone methyltransferase, DNA methyltransferase, RNA methyltransferase, and other methylation enzyme used in receptor study datasets.
- JAVA_code_examples: Java codes.
- JAVA_code_examples: input_files_to_codes.

- Supplementary_data: neural_network_inputs and neural_network_outputs (small_RNA, receptor_virus_non_virus, receptor_cell_memb_nuclear, and receptor_NMD_non_NMD)

References

1. Chariker JH, Miller DM, Rouchka EC. Computational Analysis of G-Quadruplex Forming Sequences across Chromosomes Reveals High Density Patterns Near the Terminal Ends. PLoS One. 2016 Oct 24;11(10):e0165101.

2. Scholz A, Eggenhofer F, Gelhausen R, Grüning B, Zarnack K, Brüne B, Backofen R, Schmid T. uORF-Tools-Workflow for the determination of translation-regulatory upstream open reading frames. PLoS One. 2019 Sep 12;14(9):e0222459.

3. Zhao J, Li Y, Wang C, Zhang H, Zhang H, Jiang B, Guo X, Song X. IRESbase: A Comprehensive Database of Experimentally Validated Internal Ribosome Entry Sites. Genom. Proteom. Bioinform. 18(2): 129-139 (2020).

4. Choi S. H. , Heo K. , Byun H. M. , An W. , Lu W. , Yang A. S. (2011). Identification of preferential target sites for human DNA methyltransferases. Nucleic Acids Research, 39, 104–118. 10.1093/nar/gkq774

5. Liu H, Wang H, Wei Z, Zhang S, Hua G, Zhang SW, et al. MeT-DB V2.0: elucidating context-specific functions of N6-methyl-adenosine methyltranscriptome. Nucleic Acids Res. 2018;46(D1):D281–D2D7.

6. Kuksa PP, Amlie-Wolf A, Katanic´ Z˘ , Valladares O, Wang LS, Leung YY. DASHR 2.0: integrated database of human small non-coding RNA genes and mature products. Bioinformatics. 2019 Mar 15;35(6):1033-1039.

7. Smit, AFA, Hubley, R & Green, P. RepeatMasker Open-4.0. 2013-2015 <http://www.repeatmasker.org>.

8. Kaplan OI, Berber B, Hekim N, Doluca O. G-quadruplex prediction in E. coli genome reveals a conserved putative G-quadruplex-Hairpin-Duplex switch. Nucleic Acids Res. 2016 Nov 2; 44(19): 9083–9095.

9. Mukherjee AK, Sharma S, Chowdhury S. Non-duplex G-Quadruplex Structures Emerge as Mediators of Epigenetic Modifications. Trends Genet. 2019 Feb;35(2):129-144.
10. Somers J, Pöyry T, Willis AE. A perspective on mammalian upstream open reading frame function. Int J Biochem Cell Biol. 2013 Aug;45(8):1690-700.
11. Baldrich P, Campo S, Wu MT, Liu TT, Hsing YI, San Segundo B. MicroRNA-mediated regulation of gene expression in the response of rice plants to fungal elicitors. RNA Biol. 2015;12(8):847-63.
12. Baldrich P, Campo S, Wu MT, Liu TT, Hsing YI, San Segundo B. MicroRNA-mediated regulation of gene expression in the response of rice plants to fungal elicitors. RNA Biol. 2015;12(8):847-63.
13. Alexandrova J, Paulus C, Rudinger-Thirion J, Jossinet F, Frugier M. Elaborate uORF/IRES features control expression and localization of human glycyl-tRNA synthetase. RNA Biol. 2015 Dec; 12(12): 1301–1313.
14. Aravin AA, Sachidanandam R, Bourc'his D, Schaefer C, Pezic D, Toth KF, Bestor T, Hannon GJ. A piRNA pathway primed by individual transposons is linked to de novo DNA methylation in mice. Mol Cell. 2008 Sep 26;31(6):785-99.
15. Pasero P, Bensimon A, Schwob E. Single-molecule analysis reveals clustering and epigenetic regulation of replication origins at the yeast rDNA locus. Genes Dev. 2002 Oct 1;16(19):2479-84.
16. Morales L, Oliveros JC, Fernandez-Delgado R, tenOever BR, Enjuanes L, Sola I. SARS-CoV-Encoded Small RNAs Contribute to Infection-Associated Lung Pathology. Cell Host Microbe. 2017 Mar 8;21(3):344-355.
17. Cˇ utová M, Manta J, Porubiaková O, Kaura P, Sˇ tˇ astný J, Jagelská EB, Goswami P, Bartas M, Brázda V. Divergent distributions of inverted repeats and G-quadruplex forming sequences in Saccharomyces cerevisiae. Genomics. 2020 Mar;112(2):1897-1901.
18. Chen HY, Ma SL, Huang W, Ji L, Leung VH, Jiang H, Yao X, Tang NL. The mechanism of transactivation regulation due to polymorphic short tandem repeats (STRs) using IGF1 promoter as a model. Sci Rep. 2016 Dec 2;6:38225.

19. Kumar S, Chinnusamy V, Mohapatra T. Epigenetics of Modified DNA Bases: 5-Methylcytosine and Beyond. Front Genet. 2018;9:640.
20. Alarcón, C. R., Lee, H., Goodarzi, H., Halberg, N., and Tavazoie, S. F. (2015b). N6-methyladenosine marks primary microRNAs for processing. Nature 519, 482–485.
21. Merino GA, Raad J, Bugnon LA, Yones C, Kamenetzky L, Claus J, Ariel F, Milone DH, Stegmayer G. Novel SARS-CoV-2 encoded small RNAs in the passage to humans. Bioinformatics. 2020 Nov 27;btaa1002.
22. Morales L, Oliveros JC, Fernandez-Delgado R, tenOever BR, Enjuanes L, Sola I. SARS-CoV-Encoded Small RNAs Contribute to Infection-Associated Lung Pathology. Cell Host Microbe. 2017 Mar 8;21(3):344-355.
23. Tabansky I, Stern JN, Pfaff DW. Implications of Epigenetic Variability within a Cell Population for "Cell Type" Classification. Front Behav Neurosci. 2015 Dec 16;9:342.
24. Ravindra NG, Alfajaro MM, Gasque V, Habet V, Wei J, Filler RB, Huston NC, Wan H, Szigeti-Buck K, Wang B, Wang GQ, Montgomery RR, Eisenbarth SC, Williams AJ, Pyle AM, Iwasaki A, Horvath TL, Foxman EF, Pierce RW, van Dijk D, Wilen CB. 2020. Single-cell longitudinal analysis of SARS-CoV-2 infection in human airway epithelium. bioRxiv
25. Qi F., Qian S., Zhang S., Zhang Z. Single cell RNA sequencing of 13 human tissues identify cell types and receptors of human coronaviruses. Biochem. Biophys. Res. Commun.
26. Alumkal JJ, Herman JG. Distinct epigenetic mechanisms distinguish TMPRSS2-ERG fusion-positive and -negative prostate cancers. Cancer Dis. 2012;2:979–981.
27. Kar A., Gutierrez-Hartmann A. Molecular mechanisms of ETS transcription factor mediated tumorigenesis. Crit. Rev. Biochem. Mol. Biol. 2013;48:522–543.
28. Henkart PA. ICE family proteases: mediators of all apoptotic cell death? Immunity. 1996;4(3):195–201.
29. 3 Characterization of intergenic regions and gene definition. *Nature* (2019). https://doi.org/10.1038/nature28172
30. Eibe Frank, Mark A. Hall, and Ian H. Witten (2016). The WEKA Workbench. Online Appendix for "Data Mining: Practical Machine Learning Tools and Techniques", Morgan Kaufmann, Fourth Edition, 2016.

31. Saçar Demirci MD, Adan A. Computational analysis of microRNA-mediated interactions in SARS-CoV-2 infection. PeerJ
2020;2020:1−17.
32. Chen Y, Wang X. miRDB: an online database for prediction of functional microRNA targets. Nucleic Acids Res. 2020 Jan 8;48(D1):D127-D131.
33. Han H, Cho JW, Lee S, Yun A, Kim H, Bae D, Yang S, Kim CY, Lee M, Kim E, Lee S, Kang B, Jeong D, Kim Y, Jeon HN, Jung H, Nam S, Chung M, Kim JH, Lee I. TRRUST v2:an expanded reference database of human and mouse transcriptional regulatory interactions. Nucleic Acids Res 46(D1):D380–D386 (2018).
34. Zhang Z., Zhu Z., Chen W., Cai Z., Xu B., Tan Z., Wu A., Ge X., Guo X., Tan Z., et al. Cell membrane proteins with high N-glycosylation, high expression and multiple interaction partners are preferred by mammalian viruses as receptors. Bioinformatics. 2019;35:723–728.